Summary: We present results for the temperature and pressure dependence of local structure and chain packing in *cis*-1,4-polybutadiene (*cis*-1,4-PB) from detailed molecular dynamics (MD) simulations with a united-atom model. The simulations have been executed in the NPT statistical ensemble with a parallel, multiple time step MD algorithm, which allowed us to access simulation times up to 1 μs. Because of this, a 32 chain C_{128} *cis*-1,4-PB system was successfully simulated over a wide range of temperature (from 430 to 195 K) and pressure (from 1 atm to 3 kbar) conditions. Simulation predictions are reported for the temperature and pressure dependence of the: (a) density; (b) chain characteristic ratio, C_n; (c) intermolecular pair distribution function, $g(r)$, static structure factor, $S(q)$, and first peak position, Q_{max}, in the $S(q)$ pattern; (d) free volume around each monomer unit along a chain for the simulated polymer system. These were thoroughly compared against available experimental data. One of the most important findings of this work is that the component of the $S(q)$ vs. q plot representing intramolecular contributions in a fully deuterated *cis*-1,4-PB sample exhibits a monotonic decrease with q which remains completely unaffected by the pressure. In contrast, the intermolecular contribution exhibits a distinct peak (at around 1.4 $Å^{-1}$) whose position shifts towards higher q values as the pressure is raised, accompanied by a decrease in its intensity.

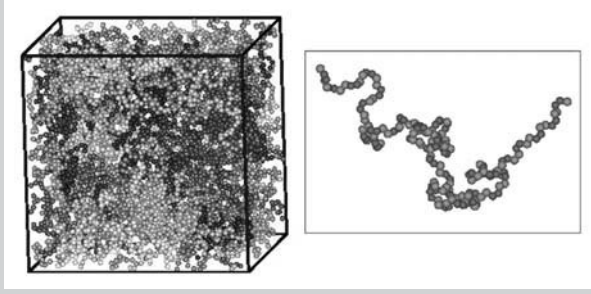

3D view of the simulation box containing 32 chains of C_{128} *cis*-1,4-polybutadiene at density $\rho = 0.849\ g \cdot cm^{-3}$ and the conformation of a single C_{128} *cis*-1,4-PB chain fully unwrapped in space.

Temperature and Pressure Effects on Local Structure and Chain Packing in *cis*-1,4-Polybutadiene from Detailed Molecular Dynamics Simulations

Georgia Tsolou,[1,2,3] *Vagelis A. Harmandaris,*[1,4] *Vlasis G. Mavrantzas**[1,2,3]

[1] Institute of Chemical Engineering and High-Temperature Chemical Processes (FORTH-ICE/HT), GR 26504 Patras, Greece
[2] University of Patras, Department of Chemical Engineering, GR 26504 Patras, Greece
Fax: +30-2610-965-223; E-mail: vlasis@chemeng.upatras.gr
[3] Interdepartmental Program of Graduate Studies on ''Polymer Science and Technology'', University of Patras, GR 26504 Patras, Greece
[4] Max Planck Institute for Polymer Research, D-55128 Mainz, Germany

Received: December 18, 2005; Revised: March 17, 2006; Accepted: March 21, 2006; DOI: 10.1002/mats.200500088

Keywords: molecular dynamics; polybutadiene; pressure; structure; static structure factor; temperature

1. Introduction

Motivated by the wide applications of polydienes, such as polybutadiene (PB) and polyisoprene (PI), in chemical technology (e.g., in the automotive and electronics industries and in rubber technology), we have recently undertaken a systematic investigation of the structure-property relationships in these two polymers through detailed simulations at the atomistic level with a united-atom model.[1,2] In ref.,[1] in particular, we presented results from very long (up to 600 ns) equilibrium MD simulations of model *cis*-1,4-PB systems, using fully equilibrated initial configurations, obtained with an efficient chain connectivity MC algorithm.[2] A similar simulation methodology had been applied in the past to predict the terminal relaxation dynamics in linear PE.[3] The simulations in all these cases had been restricted to atmospheric pressure and to temperatures above the melting point of the polymer under study (e.g., *cis*-1,4-PB and PE), addressing issues related to structural, conformational and dynamic properties, mainly as a function of chain length.

These studies are extended here to a wider range of temperature (from 430 to 195 K) and pressure (from 1 atm to 3 kbar) conditions for the *cis*-1,4-PB polymer, in an effort to study thermal and pressure (or density) effects on its structural and dynamic properties. The work is motivated by the recent experimental observations (with techniques like dielectric spectroscopy and quasielastic neutron scattering) on the influence of hydrostatic pressure on the local dynamics of polymers such as PB, 1,4-polyisoprene (PI), poly(propylene glycol) (PPG), poly(2-vinylpyridine) (P2VP), polyisobutylene (PIB)[4–11] and other glass-forming polymers at temperatures close to the glass transition temperature, T_g.[12–14] This paper discusses simulation findings for the temperature and pressure dependence of the volumetric, structural and conformational properties of *cis*-1,4-PB. Additional results about the temperature and pressure dependence of its (segmental and terminal) relaxation properties, the density and thermal contributions to its local dynamics, and its dielectric spectrum along different thermodynamic paths (isobaric, isothermal and isochoric) have been presented in a recent publication.[15]

The rest of this paper is organized as follows. Section 2 discusses the molecular model, the molecular characteristics of the simulated polymer and the temperature and pressure conditions at which the simulations were carried out. Detailed results for the thermodynamic, conformational and structural properties of the simulated system are reported in Section 3. Also reported in Section 3 are simulation results concerning the free volume in *cis*-1,4-PB, and its variation with temperature, pressure and density. The paper concludes with Section 4 discussing the major findings of the present work.

2. Molecular Model, Simulation Methodology and Systems Studied

The model used in the present simulations is the same as that employed in our recent work on the study of the static and dynamic properties of *cis*-1,4-PB in the melt state ($T \geq$ 298 K) at $P = 1$ atm.[1] It is a united atom model in which every CH_n group in the chain is represented as a single interaction site (see Figure 1), based on the descriptions proposed recently by Gee and Boyd[16] and Smith and Paul[17] from quantum chemistry calculations. Details on the force-field parameterization are given in Table 1 and will not be analyzed further. With this united-atom model, a strictly monodisperse 32 chain *cis*-1,4-PB system with 128 carbon atoms per chain (herein referred to as the C_{128} *cis*-1,4-PB system) was simulated in this paper. In all cases, the MD simulation was carried out in the isothermal-isobaric (NPT) statistical ensemble, at temperatures ranging from 430 to 195 K, and pressures ranging from 1 atm to 3 kbar (see Table 2). To also simulate the sample under isochoric conditions, the temperature and pressure conditions were carefully chosen so as to correspond (in many cases) to the same density for the simulated system. This was achieved by trial and error runs, and the (T, P) pairs located are listed in Table 3. For comparison, we mention that the experimentally accepted glass transition temperature for infinitely high *cis*-1,4-PB at $P = 1$ atm is between 160 and 175 K.[18,19] Temperature and pressure were maintained constant in the MD simulations at their prescribed values by employing the Nosé-Hoover[20,21] thermostat-barostat.

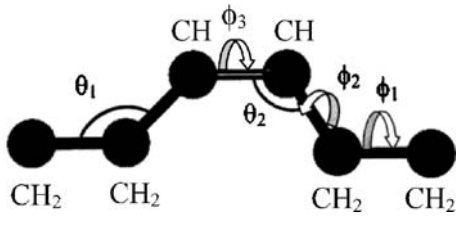

Figure 1. United atom model of *cis*-1,4-PB. The bending angles are denoted as θ_1 and θ_2 and the dihedrals as ϕ_1, ϕ_2 and ϕ_3.

An initial configuration for the simulated system was created using the Cerius^2 software[22] followed by a minimization procedure.[23] This was subsequently subjected to an exhaustive pre-equilibration run via a long NVT MD simulation at $P = 1$ atm and at a density value equal to the experimentally measured one at $T = 413$ K, followed by a long NPT MD production run at the same conditions for about 50 ns. Subsequent MD simulations at progressively lower temperatures were started from the equilibrated configurations obtained at the end of the MD simulations at a higher temperature. Similarly, fully equilibrated configurations obtained from long MD runs at low pressures were used as initial configurations for the MD runs at the higher pressures. The equations of motion were integrated using a multiple-time step algorithm (the rRESPA[24] method), with the small integration step selected equal to 1 fs and the large one equal to 5 fs, in all MD runs. The duration of the MD production runs varied from 50 ns for the higher temperatures and lower pressures up to 1 μs for the lower temperatures and higher pressures. All MD runs were carried out with the large scale atomic/molecular massively parallel simulator (LAMMPS) code[25] that can run on any parallel platform supporting the MPI library.

3. Results

A. Computational Efficiency

The fact that full equilibration of the simulated C_{128} *cis*-1,4-PB system was achieved at all length scales in the course of all NPT MD simulations of the present study is demonstrated in Figure 2 which shows the decay of the autocorrelation function $\langle \mathbf{u}(t) \cdot \mathbf{u}(0) \rangle$ of the unit vector $\mathbf{u}$ directed along the chain end-to-end vector with simulation time t, for $T = 225$ K and $P = 1$ atm, for $T = 310$ K and

Table 1. Molecular model for the *cis*-1,4-PB system (see ref.[16] and ref.[17]). For the definition of the different types of torsional angles and of the Lennard-Jones centers, the interested reader is also referred to ref.[16] and ref.[17]

Interaction	Potential Form	Parameters					
Bond Stretching	$V_{str} = \frac{1}{2}k_{str}(l - l_0)^2$	Type	k_{str} / kcal · mol^{-1} · Å^{-2}	l_0 / Å			
		1	158.5	1.54			
		2	183.8	1.50			
		3	246.9	1.34			
Bending	$V_\theta = \frac{1}{2}k_\theta(\theta - \theta_0)^2$	Type	k_θ / kcal · mol^{-1} · rad^{-2}	θ_0 / deg			
		1	115	111.65			
		2	89.4	125.89			
Torsion	$U(\phi) = \frac{1}{2}\sum_{n=1}^{6} k_n(1 - \cos(n\phi))$	Type	k_1 / kcal · mol^{-1}	k_2 / kcal · mol^{-1}	k_3 / kcal · mol^{-1}	k_4 / kcal · mol^{-1}	k_5 / kcal · mol^{-1}	k_6 / kcal · mol^{-1}
		3	–	24.2	–	–	–	–
		2	1.033	−0.472	0.554	0.263	0.346	0.164
		1	−0.888	−0.619	−3.639	−0.066	−0.247	−0.190
Nonbond	$V_{ij} = 4\varepsilon\left[\left(\frac{\sigma}{r_{ij}}\right)^{12} - \left(\frac{\sigma}{r_{ij}}\right)^{6}\right]$	Type	ε / kcal · mol^{-1}				r_{min} / Å	
		1	0.0936				4.500	
		2	0.1000				3.800	
		3	0.1015				4.257	

$P = 2.5$ kbar and for $T = 380$ K and $P = 3.0$ kbar. It can be seen that by extending the MD simulations out to times of the order of microseconds, $\langle \mathbf{u}(t) \cdot \mathbf{u}(0) \rangle$ approaches the zero value in almost all of these three cases, demonstrating excellent equilibration of the system long length scale orientational characteristics. Also remarkable is the equilibration of the average chain dimensions under these conditions, as demonstrated in Figure 3 for the relaxation of the instantaneous values of the mean-square chain end-to-end distance, $\langle R^2 \rangle$, and of the mean square radius of gyration, $\langle R_g^2 \rangle$, for the simulated system, at $T = 225$ K and $P = 1$ atm. After a short equilibration period (which should be commensurate with the longest relaxation time at the temperature and pressure conditions of the simulation), both $\langle R^2 \rangle$ and $\langle R_g^2 \rangle$ are observed to fluctuate around a constant average value, which is indicative of a fully relaxed system. Additional results on the temperature and pressure dependence of the average chain dimensions are reported in Section 3(C) below.

The fact that truly bulk polymer models of *cis*-1,4-PB have been successfully simulated over such a broad range of pressures and temperatures (going down to within a few degrees of its glass transition temperature) is very significant, since it opens up a way to simulate the glass transition phenomenon itself for this polymer (*cis*-1,4-PB), which will be an outstanding achievement. It can also be used to test the validity of free volume theories and energy landscape models for the dynamics of glass-forming

Table 2. Temperature and pressure conditions at which the C_{128} *cis*-1,4-PB system was simulated.

T / K	P / kbar
195	1.013×10^{-3}
225	1.013×10^{-3}
270	1.013×10^{-3}, 0.5, 1.0, 2.5
310	1.013×10^{-3}, 1.5, 2.5
343	1.013×10^{-3}, 1.0, 1.5, 2.0, 2.5
380	1.013×10^{-3}, 1.0, 1.5, 2.0, 2.5, 3.0
413	1.013×10^{-3}, 1.0, 1.5, 2.0, 2.5, 3.0
430	1.013×10^{-3}, 1.0, 1.5, 2.0, 2.5, 3.0

Table 3. Different temperature and pressure pairs corresponding to the same density for the C_{128} *cis*-1,4-PB system.

Density / g · cm^{-3}	T / K	P / kbar
0.94 ± 0.01	270	1.013×10^{-3}
	413	1.5
0.97 ± 0.01	225	1.013×10^{-3}
	270	0.5
	343	1.5
	380	2
	430	2.5
0.98 ± 0.01	310	1.5
	343	2
	380	2.5
	430	3.0

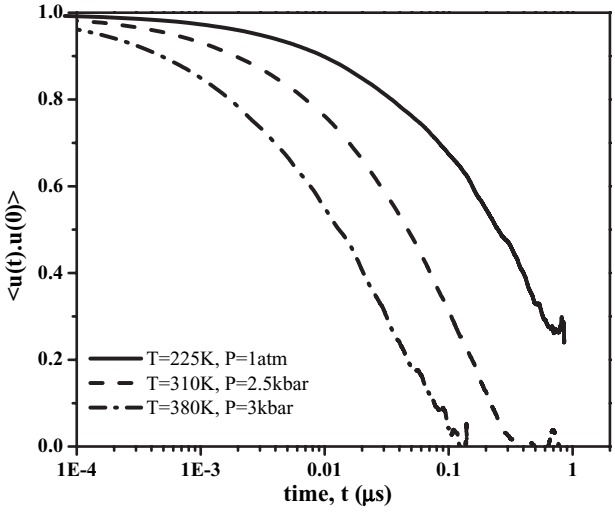

Figure 2. Decay of the chain end-to-end vector orientational autocorrelation function $\langle \mathbf{u}(t) \cdot \mathbf{u}(0) \rangle$ with simulation time t, as obtained from the present NPT MD simulations with the C_{128} *cis*-1,4-PB system, at different pressure and temperature conditions.

materials. Results from these latest efforts will be communicated in a forthcoming publication.

B. Thermodynamic Properties

Figure 4 and 5 present the dependence of the specific volume, υ, of the simulated C_{128} *cis*-1,4-PB system on temperature, T, and pressure, P. In particular, Figure 4 shows the variation of υ with T under isobaric conditions, while Figure 5 the variation of υ with P under isothermal conditions. Our simulation data for different isobars in the range 1 atm–3 kbar show that: (a) υ increases linearly as T is increased along an isobar; (b) υ decreases faster than linearly when the system is isothermally compressed. In the literature,[26–29] a common way of describing the pressure-volume-temperature (*PVT*) dependencies of amorphous polymers is through the use of the empirical Tait equation:

$$\upsilon(P,T) = \upsilon(0,T)\left\{1 - C\ln\left[1 + \frac{P}{B(T)}\right]\right\} \tag{1}$$

where the parameter C is a constant equal to 0.0894, the temperature T is in °C and the functions $\upsilon(0,T)$ and $B(T)$ are given through:

$$\upsilon(0,T) = \upsilon_0 \exp(aT) \tag{2a}$$

or, for small enough values of a, through

$$\upsilon(0,T) \cong \upsilon_0(1 + aT) \tag{2b}$$

and

$$B(T) = B_0 \exp(-B_1 T) \tag{3}$$

respectively. The parameter a in Equation (2a) and (2b) denotes the value of the thermal expansion coefficient, a_p, formally defined through:

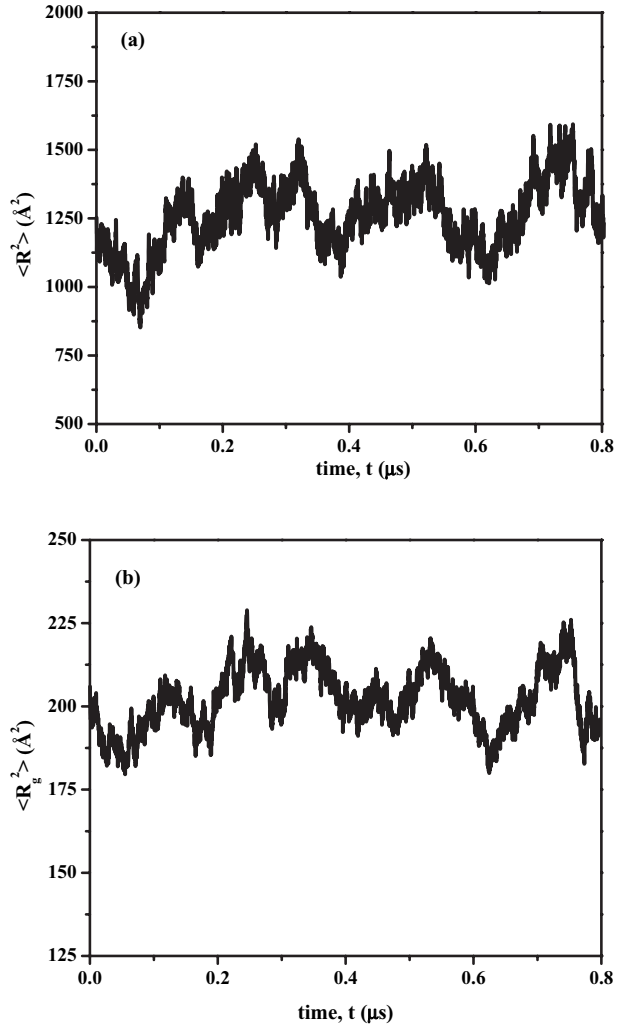

Figure 3. Running average values of (a) the mean-square end-to-end distance, $\langle R^2 \rangle$, and (b) the mean radius of gyration, $\langle R_g^2 \rangle$, with simulation time t. The results have been obtained from the present NPT MD simulations with the C_{128} *cis*-1,4-PB system at $T = 225$ K and $P = 1$ atm.

$$a_p = \frac{1}{\upsilon}\left(\frac{\partial \upsilon}{\partial T}\right)_P \tag{4}$$

at zero pressure.

Since, in the regime of temperature and pressure conditions covered in the simulations, the specific volume increases linearly with temperature along an isobar (see Figure 4), the derivative $\left.\frac{\partial \upsilon(T,P)}{\partial T}\right|_P$ is a function only of the pressure P. Consequently, for a given pressure, the thermal expansion coefficient a_p will vary with T in the same way as the inverse of the specific volume, υ, varies with T. At zero pressure, in fact, our simulation data are more consistent with Equation (2b) above than with Equation (2a), with the best fit values for a and υ_0 as follows: $a = (7.1 \pm 0.1) \times 10^{-4}$ °C^{-1} and $\upsilon_0 = (1.06 \pm 0.01)$ cm$^3 \cdot$ g^{-1}. By inserting these values in Equation (1), one can then use the Tait equation to fit the simulation data of Figure 5 along an

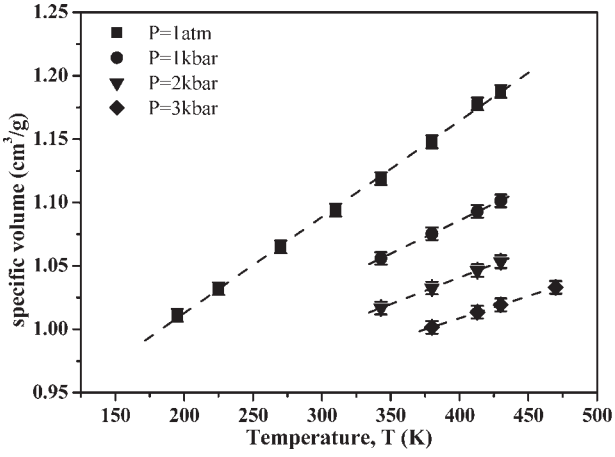

Figure 4. Temperature dependence of the specific volume, υ, for the C_{128} *cis*-1,4-PB system, at various pressures. The dashed lines correspond to linear regression fittings of the simulation data.

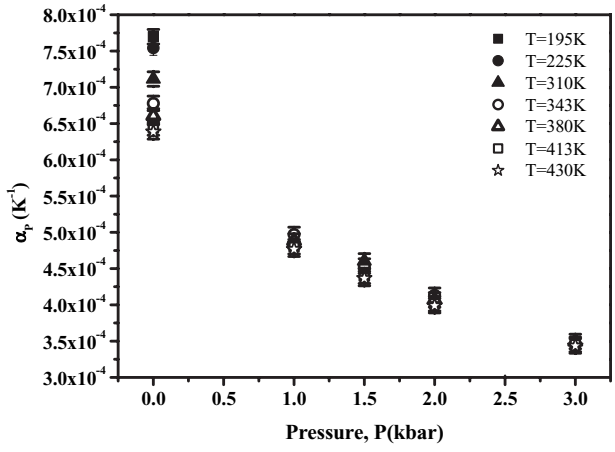

Figure 6. Pressure and temperature dependence of the thermal expansion coefficient, α_P, as calculated from the present MD simulations with the C_{128} *cis*-1,4-PB system.

isotherm with only one parameter, the temperature dependent parameter B, i.e., $B = B(T)$. By analyzing the function $B = B(T)$, one can thus check if it follows the exponential law of Equation (3) and if so, to obtain the best fit values of B_0 and B_1. Fittings of the simulation data for the *PVT* properties of the simulated *cis*-1,4-PB system with the Tait equation are shown by the dashed lines in Figure 5 and are seen to follow the simulation data remarkably accurately. It was also observed (results not shown) that the function $B(T)$ extracted from the simulation data followed the exponential form of Equation (3) astonishingly well, with the best fit values of B_0 and B_1 as follows: $B_0 = (1.45 \pm 0.02)$ kbar and $B_1 = (4.1 \pm 0.1) \times 10^{-3}\ ^\circ\mathrm{C}^{-1}$.

The variation of the thermal expansion coefficient, a_p, with temperature and pressure for the simulated system is reported in Figure 6. With increasing pressure, a_p is seen to decrease considerably (which reflects the decreasing rate of compression of the system as the pressure is raised), in excellent agreement with the experimental observations of Barlow.[28]

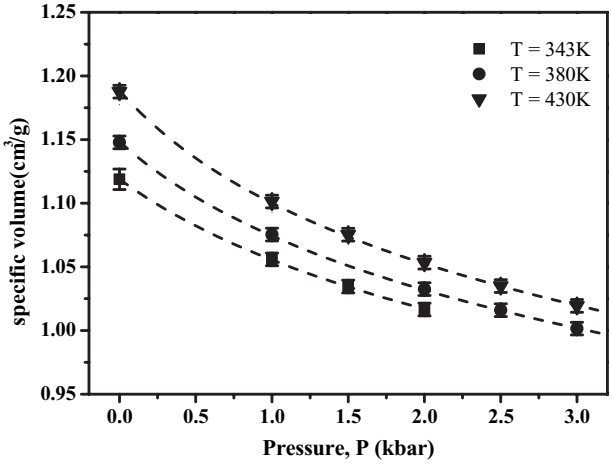

Figure 5. Pressure dependence of the specific volume, υ, for the C_{128} *cis*-1,4-PB system, at various temperatures. The dashed lines show the best fittings to the simulation results with the Tait equation (Equation (1) in the main text).

As mentioned before, the simulation prediction for a_p for the C_{128} *cis*-1,4-PB system at $P = 1$ atm depends on temperature, decreasing from $(7.7 \pm 0.1) \times 10^{-4}\ \mathrm{K}^{-1}$ at $T = 195$ K, to $(7.1 \pm 0.1) \times 10^{-4}$ at $T = 310$ K and to $(6.4 \pm 0.1) \times 10^{-4}$ at $T = 430$ K. These values are consistent with literature data reported, for example, by Paul and DiBenedetto[30,31] for a pure *cis*-1,4-PB system ($a_p = 6.7 \times 10^{-4}\ \mathrm{K}^{-1}$ at $T = 298$ K), by Smith et al.[32] for a random PB copolymer sample through ^{13}C NMR experiments and MD simulations ($a_p = 7.1 \times 10^{-4}\ \mathrm{K}^{-1}$ at $T = 353$ K), by Barlow[28] ($a_p = 7.35 \times 10^{-4}\ \mathrm{K}^{-1}$ in the temperature range 277–328 K) and by Valentine et al.[33] ($a_p = 7.5 \times 10^{-4}\ \mathrm{K}^{-1}$) for a random copolymer of PB (containing only 43% *cis*-1,4). Anderson et al.[34] have also reported a_p for a high *cis*-1,4-PB sample through NMR measurements ($a_p = 5.7 \times 10^{-4}\ \mathrm{K}^{-1}$ at $T = 296$ K).

In addition to the thermal expansion coefficient, another important thermodynamic parameter that can be obtained from the temperature and pressure dependence of the specific volume is the isothermal compressibility, κ_T, defined through the slope of the curve describing the variation of υ with P under isothermal conditions:

$$\kappa_T \equiv -\frac{1}{\upsilon}\left(\frac{\partial \upsilon}{\partial P}\right)_T \tag{5}$$

Using the above relation, κ_T can be straightforwardly extracted from the MD simulations through the υ vs. P plots of Figure 5. To avoid numerical errors associated with the calculation of the slopes of the curves shown in Figure 5, an alternative and more accurate way to calculate κ_T is through the fluctuations in the system volume, V, in the course of the

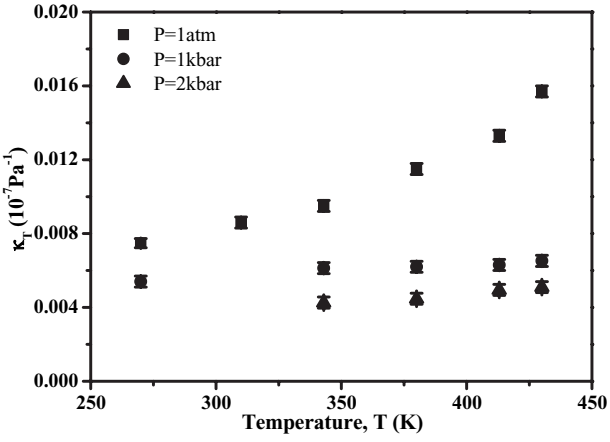

Figure 7. Temperature dependence of the isothermal compressibility, κ_T, as calculated from the present MD simulations with the C_{128} *cis*-1,4-PB system, at various pressures.

NPT MD runs, according to:[35,36]

$$\kappa_T = \frac{\langle V^2 \rangle - \langle V \rangle^2}{k_B T \langle V \rangle} \tag{6}$$

κ_T values calculated through Equation (6) for the simulated polymer as a function of temperature are reported in Figure 7. It can be observed that κ_T is practically independent of T, except at the smallest pressure studied ($P = 1$ atm) where κ_T is observed to increase with increasing T. Isothermally increasing the pressure, on the other hand, causes κ_T to decrease. As far as the numerical values of κ_T are concerned, these are fully consistent with available experimental measurements for the simulated system. For example, the simulation prediction for κ_T at $T = 270$ K is $(7.3 \pm 0.2) \times 10^{-10}$ Pa^{-1}, which coincides with the experimental value reported by DiBennedetto[31] ($\kappa_T = 7.25 \times 10^{-10}$ Pa^{-1}) for a 1,4 PB sample of unspecified microstructure at $T = 298$ K; somewhat smaller is the value reposted by Anderson et al.[34] for a high *cis*-1,4-PB sample ($\kappa_T = 3.6 \times 10^{-10}$ Pa^{-1}) at $T = 296$ K.

C. Conformational Properties

Chain conformational properties in the simulated polymer were analyzed here in terms of bending and torsion-angle distributions and chain dimension parameters, such as the mean-square end-to-end distance, $\langle R^2 \rangle$, radius of gyration, $\langle R_g^2 \rangle$, and chain characteristic ratio, C_n.

The effect of temperature on the distribution of bending and torsion angles along a *cis*-1,4-PB chain was also studied (in part) in our previous work,[1] where it was reported that, as the temperature is decreased: (a) the height of the two bending angle distributions increases; (b) the height of the two torsion-angle distributions at their peak increases; (c) the population of the *trans* state (at $\pm 180^\circ$) in the distribution of the ϕ_1 dihedral increases accompanied by an increase in the population of the two *gauche* states; (d) the *trans* population of the ϕ_2 torsion angle distribution decreases. Exactly the same observations are made in the simulations of the present study where even lower temperatures have been accessed (down to 195 K).

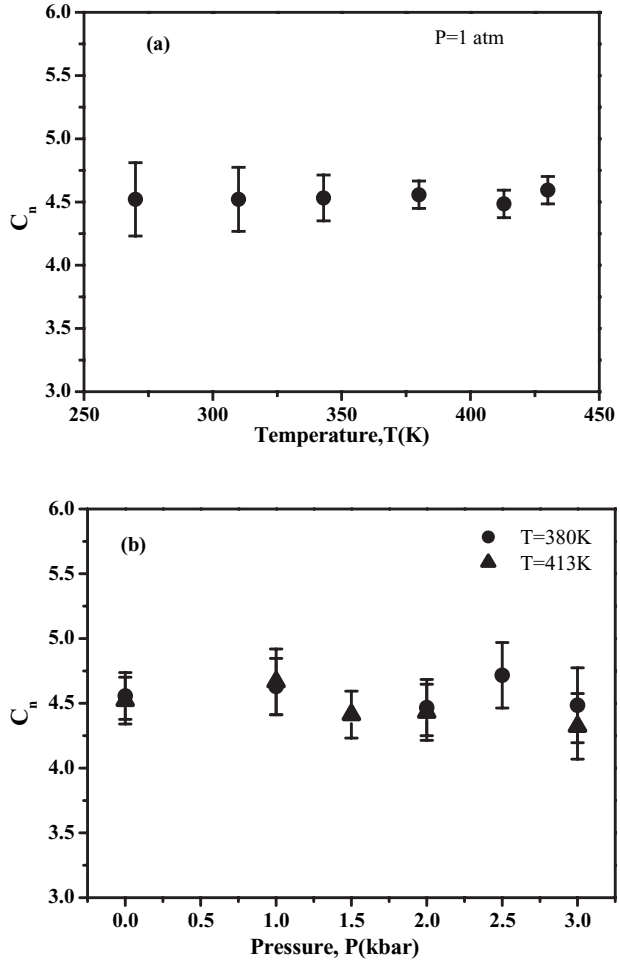

Figure 8. Dependence of the characteristic ratio, C_n, on (a) temperature (at $P = 1$ atm), and (b) pressure (at $T = 380$ and 413 K), as calculated from the present MD simulations with the C_{128} *cis*-1,4-PB system.

On the other hand, the effect of temperature and pressure on the overall size of the macromolecular chain can be discussed in terms of characteristic ratio, C_n, calculated from the simulation results for the mean-square chain end-to-end distance, $\langle R^2 \rangle$, through:

$$C_n = \frac{\langle R^2 \rangle}{n\bar{l}^2} \tag{7}$$

where n denotes the number of links in the chain backbone and $\bar{l}^2$ the average squared skeletal bond length. The temperature and pressure dependencies of C_n for the simulated polymer is presented in Figure 8(a) and 8(b). C_n is observed to remain practically constant all over the

temperature [225 K, 430 K] and pressure [1 atm, 3 kbar] ranges explored in the simulations. This result agrees well with the experimental data of Fetters et al.[37] that the ratio $\langle R^2 \rangle / M$ in 1,4 PB remains the same in the temperature range 298–413 K.

D. Structural Properties

Information about local structure in a polymeric system is provided by the intermolecular pair distribution function, $g(r)$, and/or the static structure factor, $S(q)$, which is calculated through the Fourier transform of the total pair distribution function, $g_{tot}(r)$, through:

$$S(q) = 1 + \rho N \int_0^\infty 4\pi r^2 \frac{\sin(qr)}{qr} [g_{tot}(r) - 1] dr \qquad (8)$$

where N denotes the total number of atoms and ρ the number density of the system. Although simulated $S(q)$ curves are quite difficult to compare against experimentally obtained $S(q)$ data due to a number of complicating factors and the different weightings at different q regimes in real experiments, Equation (8) provides a means for validating the predicted intermolecular pair distribution function, $g(r)$, against data obtained either from X-ray diffraction or neutron scattering measurements.[1,36,38]

The temperature dependence of $g(r)$ for the simulated *cis*-1,4-PB system is reported in Figure 9. Decreasing the temperature causes a shift of the first peak in the $g(r)$ pattern corresponding to the average position of the first intermolecular neighbors around a reference atom to smaller distances; this reflects the increase in the system density. The same happens if the pressure in increased. Figure 10, which presents $g(r)$ profiles at different pressures keeping temperature constant (equal to 310 K), shows the position of their first peak to shift to smaller distances (implying that the average position of the first intermolecular neighbors decreases) as the pressure is decreased.

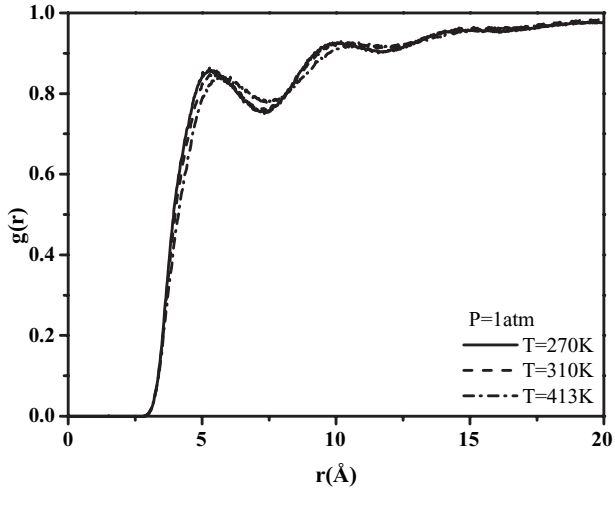

Figure 9. Intermolecular pair distribution function, $g(r)$, and its temperature dependence, as obtained from the present MD simulations with the C_{128} *cis*-1,4-PB system, at $P = 1$ atm.

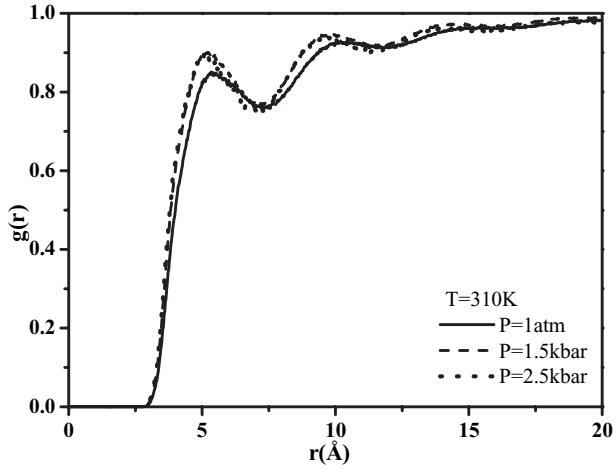

Figure 10. Intermolecular pair distribution function, $g(r)$, and its pressure variation, as obtained from the present MD simulations with the C_{128} *cis*-1,4-PB system at $T = 310$ K.

Equation (8) for the calculation of $S(q)$ is valid only if one chemical species is present in the polymer. However, most available experimental data for *cis*-1,4-PB[5,6,12,39,40] are obtained from neutron scattering techniques on polymer samples where hydrogen atoms are replaced by deuterium atoms. To take into account all different species (carbons, hydrogens and deuteriums) present in such a system, Equation (8) has to be used with hydrogen (or deuterium) atoms being introduced at their correct positions along the chain backbone following the procedure described in ref.[1] In addition, in the presence of multiple species, $S(q)$ has to be calculated from the Fourier transform of the $H(r)$ function defined through:[41]

$$H(r) = \sum_{i=1}^{2} \sum_{j=1}^{2} \frac{x_i x_j f_i f_j}{\left(\sum_{i=1}^{2} x_i f_i \right)^2} (g_{ij}(r) - 1) \qquad (9)$$

where x_i and x_j denote the number fraction of i-type (e.g., carbons) and j-type (e.g., deuterium) atoms, and f_i and f_j the respective scattering factors.

$S(q)$ vs. q plots for the simulated *cis*-1,4-PB system obtained with Equation (9) at two different temperatures (keeping P constant, equal to 1 atm) are shown by the lines in Figure 11. For comparison, also shown in the Figure (by the symbols) are experimentally measured $S(q)$ vs. q plots obtained with neutron scattering[40] techniques. The agreement between simulated and experimentally measured patterns is very satisfactory across the entire q range. Some small differences observed in the neighborhood of the

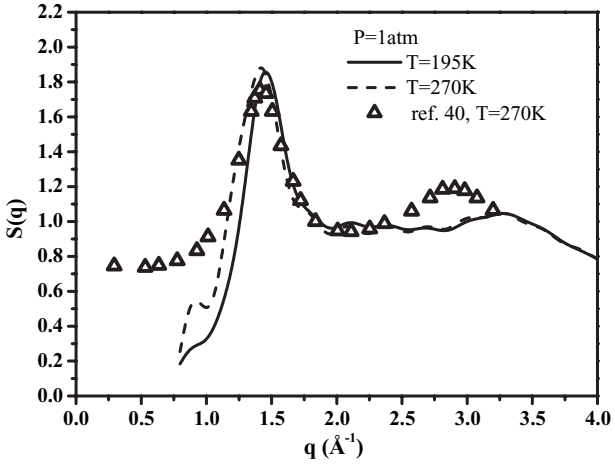

Figure 11. The static structure factor, $S(q)$, of the simulated C_{128} *cis*-1,4-PB system, as obtained from the present MD simulations at $T = 195$ K (solid line) and $T = 270$ K (dashed line), and comparison with the experimental data (triangles) of ref.[40] at $T = 270$ K. In all cases, $P = 1$ atm.

second peak are attributed to the different microstructure of the 1,4 PB sample used in the neutron scattering measurements containing a significant proportion of *trans* and vinyl units.[1] Figure 11 demonstrates that temperature affects only the position of the first peak; in contrast, the position of the second peak remains unchanged with *T*. By further analyzing the temperature dependence of the first peak position, it can be concluded that, as the temperature is decreased, this shifts towards larger q values (corresponding to smaller characteristic intermolecular distances), which mirrors the density increase and the tighter packing. The shift of the first peak position, Q_{max}, towards lower values with increasing temperature is demonstrated in Figure 12, where it is observed that Q_{max} changes almost linearly with temperature, in the temperature range studied.

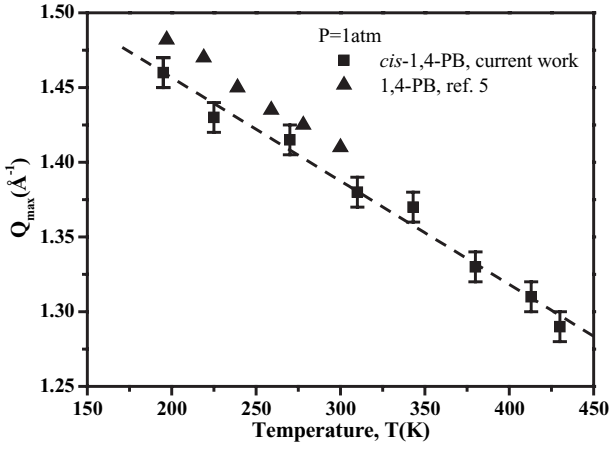

Figure 12. Temperature dependence of the first peak position, Q_{max}, in the $S(q)$ pattern for the C_{128} *cis*-1,4-PB, at $P = 1$ atm. Also shown by the filled triangles are the experimental data of ref.[5] obtained on a 1,4-PB sample.

The shift of Q_{max} under different temperature and pressure conditions has been investigated by Cailliaux et al.[6] via neutron scattering and calorimetry measurements on a 1,4-PB sample. According to the arguments put forward by Cailliaux et al.,[6] the position of Q_{max} is directly related to the system density, therefore, a sharp change should be expected in the slope of the curve describing its variation with temperature near T_g. No such change is observed here, most probably due to the fact that the lowest temperature explored (195 K) is well above the corresponding glass transition temperature; this issue will be revisited in a forthcoming contribution.

Frick et al.[5] have suggested that, if one accepts that the first peak position reflects to a large extent intermolecular correlations, then one can deduce a *linear thermal expansion coefficient* from the slope of the curve describing the temperature dependence of Q_{max} through:

$$\beta = \left(1/Q_{max}\right)\left(\partial Q_{max}/\partial T\right)_P \tag{10}$$

Based on such a definition for β, the value for the linear thermal expansion coefficient obtained from our simulations with the C_{128} *cis*-1,4-PB system at $T = 310$ K is $\beta = (4.95 \pm 0.05) \times 10^{-4}$ K^{-1}. Usually, the value of *the linear expansion coefficient* β is smaller than that of *the true thermal expansion coefficient* α_P calculated from the volumetric data. Earlier literature data[42] support that $\alpha_P \approx 3\beta$, while more recent neutron scattering experiments suggest that α_P should be only slightly larger than β.[5,39] The latter conclusion agrees better with our results.

Pressure effects on $S(q)$ are examined in Figure 13 showing $S(q)$ vs. q plots at three different pressures under isothermal conditions ($T = 380$ K). In qualitative agreement with the temperature variations described above, as pressure increases (i.e., as density increases), the position of the first peak, Q_{max}, shifts to higher values (smaller distances), while that of the second peak remains unchanged. It is also observed that with increasing pressure, the height of the first peak in the $S(q)$ pattern for the C_{128} *cis*-1,4-PB system decreases. To analyze the origin of this behavior, we calculated the relative contributions to the $S(q)$ vs. q patterns representing intra- and intermolecular correlations from our MD simulations at $T = 413$ K using:

$$H_{ij}^{intra} = \sum_{i=1}^{2}\sum_{j=1}^{2} \frac{x_i x_j f_i f_j}{\left(\sum_{i=1}^{2} x_i f_i\right)^2} g_{ij}^{intra},$$
$$H_{ij}^{inter} = \sum_{i=1}^{2}\sum_{j=1}^{2} \frac{x_i x_j f_i f_j}{\left(\sum_{i=1}^{2} x_i f_i\right)^2} (g_{ij}^{inter} - 1) \tag{11}$$

implying that $S(q)$ can be written as the sum of intra- and inter-molecular contributions:

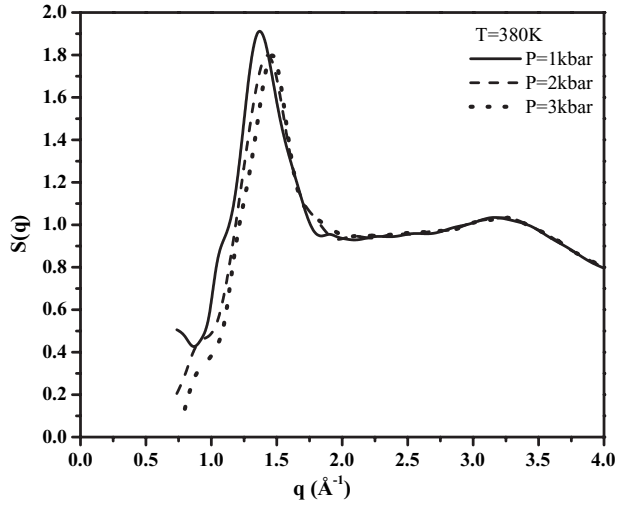

Figure 13. Pressure variation of the static structure factor, $S(q)$, for the simulated C_{128} *cis*-1,4-PB system as obtained from the present MD simulations, at $T = 380$ K.

$$S(q) = S_{\text{intra}}(q) + S_{\text{inter}}(q) \tag{12}$$

The results for two different simulation pressures, $P = 1$ atm and $P = 2.5$ kbar, are shown in Figure 14(a) and 14(b), corroborating that:

- the first peak in the $S(q)$ vs. q profile has significant contributions from both intra- and intermolecular correlations; furthermore, its shift to higher q values with increasing pressure is accompanied by an decrease in its height.
- the curve representing the intensity of the intramolecular contribution, $S_{\text{intra}}(q)$, exhibits a monotonic decrease with q, and is not affected by the pressure. In contrast, the intermolecular contribution, $S_{\text{inter}}(q)$, exhibits a distinct peak whose position shifts towards higher q values as the pressure is raised.
- the shift of the first peak of the intermolecular contribution to higher q values with increasing pressure is accompanied by an increase in its height, and
- with increasing pressure the position of the peak of the intermolecular contribution shifts to higher q values, i.e., in the regime where the contribution of the intra part is much smaller, the net result being a decrease in the intensity of the first peak in the total $S(q)$ vs. q profile with increasing pressure.

The intermolecular contribution to the static structure factor, $S_{\text{inter}}(q)$, can further be separated into contributions reflecting intermolecular correlations between carbon and deuterium atoms, as shown in Figure 15. It is observed that the component of the curve reflecting intermolecular correlations between carbon atoms, $S^{CC}_{\text{inter}}(q)$, exhibits a peak at around 1.4 Å^{-1}. The position of this peak shifts towards higher q values as P is increased; simultaneously,

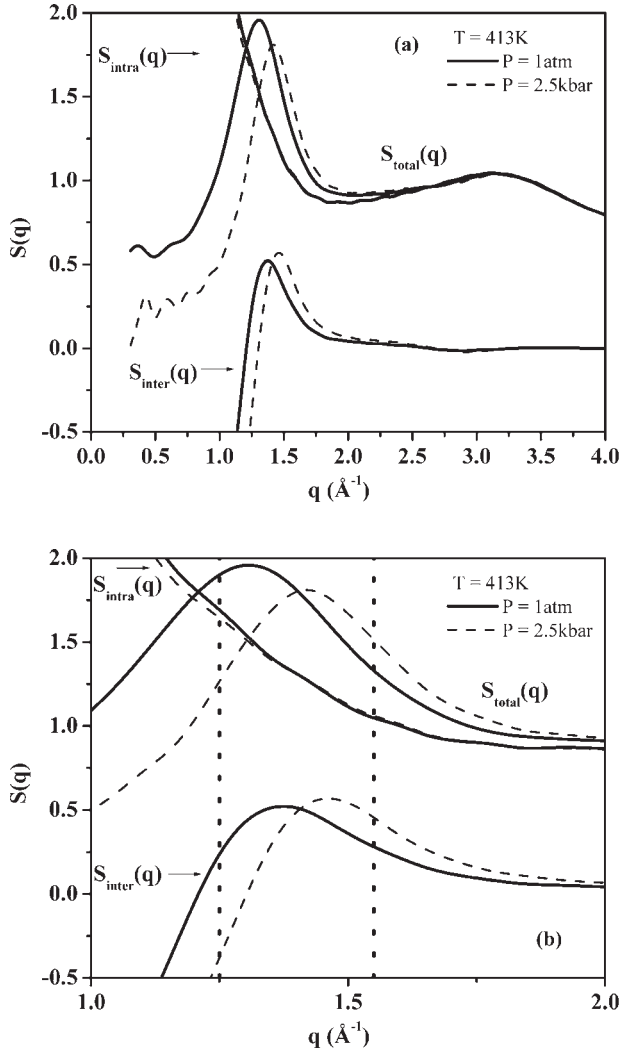

Figure 14. (a) Intramolecular and intermolecular contributions to the total structure factor, $S(q)$, for the simulated C_{128} *cis*-1,4-PB system at $P = 1$ atm (solid lines) and at $P = 2.5$ kbar (dashed lines). In all cases, $T = 413$ K. (b) Same as (a) but focusing on the region (bracketed by the dashed vertical lines) of q values around the first peak in the S(q) vs. q plot.

its height increases. The component of the curve reflecting intermolecular correlations between carbon and deuterium atoms, $S^{CD}_{\text{inter}}(q)$, also exhibits a peak, but a less intense one, at around 1.4 Å^{-1}, whose position moves again to higher q values as P is increased.

That the position of the first peak $S(q)$ vs. q pattern shifts towards higher q values as P is increased (followed by an increase in its height) is one of the most significant results of the present simulation study. In fact, similar conclusions have been very recently reported also by Narros et al.[43] who investigated the short range order in 1,4-PB with a chain microstructure composed of 53% *trans*, 39% *cis* and 8% vinyl units, by combining fully atomistic MD

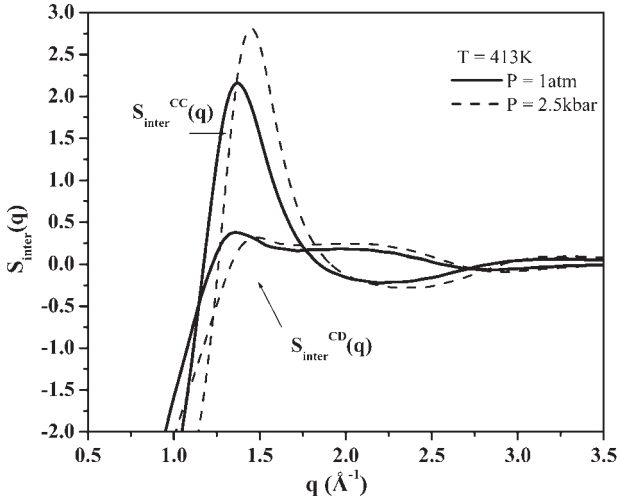

Figure 15. Decomposition of the intermolecular part of the total structure factor, $S(q)$, for the simulated *cis*-1,4-PB system to contributions from carbon-carbon and carbon-deuterium correlations at $P = 1$ atm (solid lines) and $P = 2.5$ kbar (dashed lines) [$T = 413$ K].

simulations and neutron diffraction with polarization analysis on isotopically labeled samples. In fact, Narros et al.[43] found that although the structure factor corresponding to a fully deuterated sample and the partial structure factor of the fully protonated polymer exhibit their first main peak at very similar positions (centered at about 1.4 and 1.5 $Å^{-1}$, respectively), their intensity exhibits opposite tendencies with varying temperature: in the fully deuterated sample, the intensity increases somewhat upon heating whereas in the protonated one it decreases.

Additional results for the pressure dependence of the first peak position, Q_{max}, for the simulated *cis*-1,4-PB system are reported in Figure 16, demonstrating a linear dependence of its shift with pressure. Following Cailliaux et al.,[6] a sharp change in the slope of the curves of Figure 16 would reveal a transition of the system to the glassy state once P exceeds a critical value denoted by P_g. Such behavior has indeed been reported by Cailliaux et al.[6] for the case of a high molecular weight 1,4-PB sample ($MW > 7\,000$ g · mol^{-1}) through neutron scattering and calorimetry measurements when the applied pressure exceeded $P_g = 1\,400$ MPa (for $T = 295$ K). No such critical behavior was observed in the present simulation studies in the regime of pressures accessed (and for $T \geq 270$ K).

The curves shown in Figure 16 can be further analyzed to define a *microscopic isothermal compressibility*, κ_T, through:[5] $\kappa_T = (1/Q_{max})(\partial Q_{max}/\partial P)_T$. The value obtained for the C_{128} *cis*-1,4-PB system at $T = 310$ K is $\kappa_T = (3.70 \pm 0.05) \times 10^{-4}$ MPa^{-1}. This is more than 2 times smaller than the corresponding value ($(8.60 \pm 0.05) \times 10^{-4}$ MPa^{-1}) predicted from the simulation data on the basis of volume fluctuations (see Equation (6)) at the same temperature.

Guided by the experimental observations of Frick et al.[5] that the static structure factor of a 1,4-PB system is almost identical along isochors, Figure 17 shows the variation of Q_{max} under different T and P conditions, some of which have been chosen to correspond to the same system density (see Table 3). It can be observed that:

- Q_{max} shifts linearly to higher values with increasing density, and
- Q_{max} is practically invariant (within the statistical error of the simulation results) to isochoric changes (changes in pressure and temperature along a constant density thermodynamic path), in full agreement with the experimental observations of Frick et al.[5] and the very recent studies of Narros et al.[43]

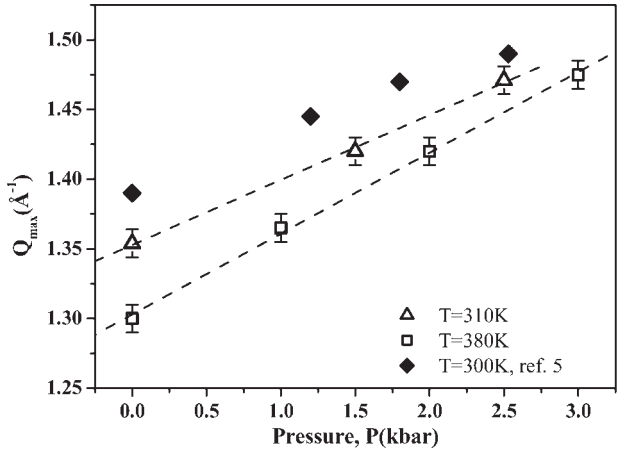

Figure 16. Pressure dependence of the first peak position, Q_{max}, in the $S(q)$ pattern for the C_{128} *cis*-1,4-PB system at $T = 310$ K (open triangles) and $T = 380$ K (open squares) plotted together with the experimental data of ref.[5] (filled diamonds).

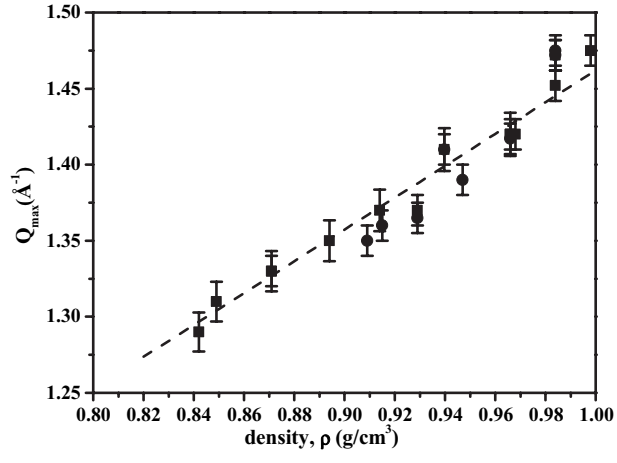

Figure 17. Density dependence of the first peak position, Q_{max}, in the $S(q)$ pattern for the C_{128} *cis*-1,4-PB system, at different pressure and temperature conditions.

E. Free Volume

Taking into consideration that changes in the system density can be driven either by decreasing the temperature or by increasing the pressure, analyzing the dependence of free volume around each polymer atom on temperature and pressure variations can yield useful information about the role played by the two thermodynamic variables (pressure and temperature) on polymer relaxation. Following the geometric analysis proposed by Greenfield and Theodorou,[44] one can calculate the free volume around a polymer atom by: (a) conducting a tessellation of space into Delaunay tetrahedral and considering the center of every Lennard-Jones (LJ) unit as a point in space [a Delaunay tetrahedron corresponds to four neighboring atoms surrounding a small ''hole'' in the bulk polymer]; (b) increasing the size of each polymer atom to its corresponding van der Waals radius ($r = 2^{1/6}(\sigma/2)$); (c) calculating the empty space inside each Delaunay tetrahedron. The unoccupied volume corresponding to each atom is calculated by summing the unoccupied volumes of all tetrahedral in which the reference atom participates. The method has been successfully applied so far in free volume and excess chain-end free volume calculations within systems such as poly(propylene),[44] small *n*-alkane and *cis*-1,4-PI oligomer melts[45] and poly(terephthalic ethylester) glasses.[46]

The free volume around each monomer in the simulated *cis*-1,4-PB system as a function of monomer position along the chain and its variation under isothermal conditions are reported in Figure 18. Clearly, the distribution of free volume is symmetric with respect to the chain midpoint. Furthermore, the free volume around chain ends is significantly higher than the free volume around inner monomers along the chain; this is due to the non-connectivity of chain ends. Further analysis reveals that in a *cis*-1,4-PB monomer, the free volume around a CH_2 group is larger than around a CH group.

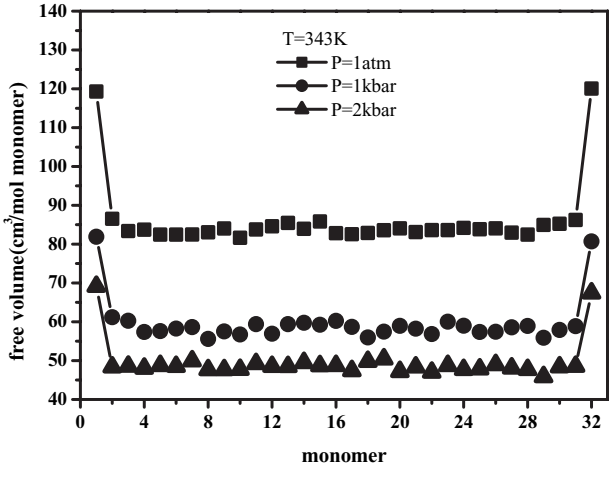

Figure 18. Typical free volume distributions as a function of monomer position along the chain backbone of the C_{128} *cis*-1,4-PB, as a function of pressure (keeping temperature constant).

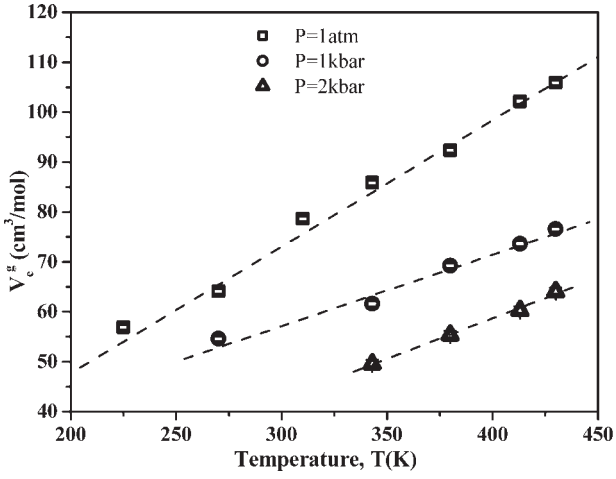

Figure 19. Temperature dependence of the total free volume around a monomer unit in the C_{128} *cis*-1,4-PB, at different pressure values. The dashed lines correspond to linear regressions of the simulation results.

The free volume varies significantly with temperature and pressure. Figure 19 and 20 show that the total free volume around a monomer unit, V_e^g, decreases as the temperature is lowered under isobaric conditions or as the pressure is increased under isothermal conditions, reflecting in both cases the increase in the system density and the tighter segmental packing. It is also interesting to note that the slope of the isobaric curve describing the temperature dependence of total free volume decreases with increasing pressure: by raising *P* from 1 atm to 2 kbar (see Figure 19), the slope decreases by 60%. As far as the variation of free

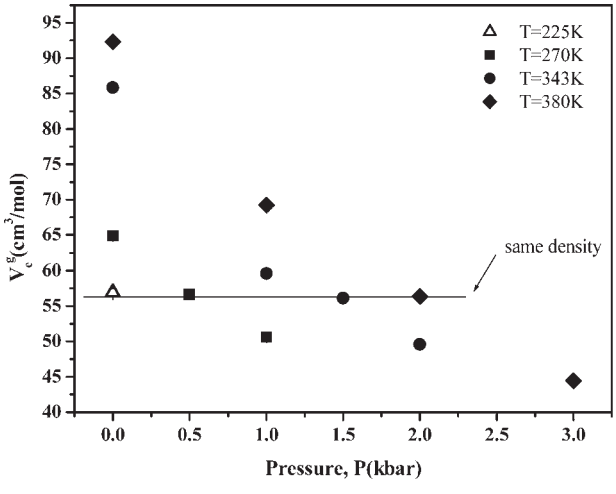

Figure 20. Pressure dependence of the total free volume around a monomer unit in the C_{128} *cis*-1,4-PB, at different temperature values. The solid line is used as eye guide to mark isochoric conditions.

volume with pressure (under isothermal conditions) is concerned, Figure 19 shows it to change non-linearly, following practically the corresponding change of specific volume with pressure (see Figure 5). In fact, if one plots the average free volume under isochoric conditions (solid line in Figure 20), i.e., under different (T, P) conditions that are characterized by the same density, then a straight line with slope equal to zero is obtained, undoubtedly demonstrating that, for a given polymer, the total free volume is solely determined by its density.

4. Conclusion

We have successfully simulated truly bulk models of *cis*-1,4-PB over a broad range of pressures and temperatures (going down to within a few degrees of its glass transition temperature) with a multiple time step MD algorithm, which allowed us to access simulation times of the order of microseconds. Apart from opening up the way towards simulating the glass transition phenomenon itself for this polymer, these microsecond long MD simulations have allowed us to analyze and obtain useful predictions for the temperature and (mainly) pressure dependencies of specific volume, chain characteristic ratio, intermolecular pair distribution function, static structure factor, first peak position in the $S(q)$ pattern and free volume around each monomer unit in a *cis*-1,4-PB system.

The specific volume was found to vary linearly with temperature under isobaric conditions, when the reference pressure varied from 1 atm to 3 kbar. Furthermore, its pressure dependence under isothermal conditions was observed to be accurately described by the empirical Tait equation. The effect of temperature and pressure on the conformation of the simulated polymer was also examined through calculations of the bending and torsion-angle distributions and chain characteristic ratio; the latter was observed to remain invariant to temperature and pressure changes.

Structural aspects in the simulated *cis*-1,4-PB system were evaluated by calculating the $g(r)$ vs. r and $S(q)$ vs. q curves under isobaric and isothermal conditions. The first peak in the $S(q)$ vs. q curve was found to shift to lower q values as the density of the system was decreased independently of the thermodynamic path followed (increase in temperature under isobaric conditions or decrease in pressure under isothermal conditions). Furthermore, its height was found to decrease when the pressure was increased.

Simulation predictions for the average free volume around a monomer unit along a *cis*-1,4-PB chain showed it to decrease under either isothermal compression (by increasing the pressure) or isobaric compression (by decreasing the temperature) following the change in the system density in both cases. Different T and P points along an isochoric were found to be characterized by exactly the same (average value of) free volume for the given polymeric sample.

Acknowledgements: Financial support from the *Greek Secretariat for Research and Technology* (GSRT) through the *AKMON programme* (Title: Design of heterogeneous materials for new applications in technologies of energy and environment, Code No: 61) is gratefully acknowledged. Very helpful discussions with Prof. *Doros Theodorou* and Prof. *George Floudas* are also greatly appreciated.

[1] [1a] G. Tsolou, V. G. Mavrantzas, D. N. Theodorou, *Macromolecules* **2005**, *38*, 1478; [1b] M. Doxastakis, V. G. Mavrantzas, D. N. Theodorou, *J. Chem. Phys.* **2001**, *115*, 11339; [1c] M. Doxastakis, V. G. Mavrantzas, D. N. Theodorou, *J. Chem. Phys.* **2001**, *115*, 11352.
[2] P. Gestoso, E. Nicol, M. Doxastakis, D. N. Theodorou, *Macromolecules* **2003**, *36*, 6925.
[3] V. A. Harmandaris, V. G. Mavrantzas, D. N. Theodorou, M. Kröger, J. Ramírez, H. C. Öttinger, D. Vlassopoulos, *Macromolecules* **2003**, *36*, 1376.
[4] B. Frick, G. Dosseh, G. A. Cailliaux, C. Alba-Simionesco, *Chem. Phys.* **2003**, *292*, 311.
[5] B. Frick, C. Alba-Simionesco, K. H. Andersen, L. Willner, *Phys. Rev. E* **2003**, *67*, 051801.
[6] A. Cailliaux, C. Alba-Simionesco, B. Frick, L. Willner, I. Goncharenko, *Phys. Rev. E* **2003**, *67*, 010802.
[7] [7a] G. Floudas, T. Reisinger, *J. Chem. Phys.* **1999**, *111*, 5201; [7b] G. Floudas, C. Gravalides, T. Reisinger, G. Wegner, *J. Chem. Phys.* **1999**, *111*, 9847.
[8] P. Papadopoulos, D. Peristeraki, G. Floudas, G. Koutalas, N. Hadjichristidis, *Macromolecules* **2004**, *37*, 8116.
[9] [9a] A. Kirpatch, D. B. Adolf, *Macromolecules* **2004**, *37*, 1576; [9b] B. J. Punchard, D. B. Adolf, *J. Chem. Phys.* **2002**, *117*, 7774.
[10] [10a] C. M. Roland, R. Casalini, T. Psurek, S. Pawlus, M. Paluch, *J. Polym. Sci., Part B: Polym. Phys.* **2003**, *41*, 3047; [10b] M. Paluch, S. Pawlus, C. M. Roland, *Macromolecules* **2002**, *35*, 7338.
[11] R. Casalini, C. M. Roland, *Colloid Polym. Sci.* **2004**, *283*, 107.
[12] B. Frick, D. Richter, *Science* **1995**, *267*, 1939.
[13] K. L. Ngai, ''The Glass Transition and the Glassy State'', in: *Physical Properties of Polymers*, 3rd edition, J. Mark, K. Ngai, W. Graessley, L. Mandelkern, E. Samulski, J. Koenig, G. Wignall, Eds., Cambridge University Press, Cambridge 2004, p. 72.
[14] [14a] G. Williams, *Trans. Faraday Soc.* **1965**, *61*, 1564; [14b] G. Williams, *Trans. Faraday. Soc.* **1965**, *62*, 2091; [14c] H. Sasabe, S. Saito, *J. Polym. Sci. A1* **1968**, *6*, 1401.
[15] G. Tsolou, V. A. Harmandaris, V. G. Mavrantzas, *J. Chem. Phys.* **2006**, *124*, 084906.
[16] R. H. Gee, R. H. Boyd, *J. Chem. Phys.* **1994**, *101*, 8028.
[17] G. D. Smith, W. Paul, *J. Phys. Chem. A* **1998**, *102*, 1200.
[18] H. L. Stephens, ''Physical Constants of Poly(butadiene)'', in: *Polymer Handbook*, 3rd edition, J. Brandup, E. H. Immergut, Eds., J. Wiley & Sons, New York 1989, p. V1.
[19] J. E. Mark, ''*Polymer Data Handbook*'', Oxford University Press, New York 1999.
[20] S. Nosé, *Mol. Phys.* **1984**, *52*, 255.
[21] W. G. Hoover, *Phys. Rev. A* **1985**, *31*, 1695.

[22] www.accelrys.com/cerius2/
[23] D. N. Theodorou, U. W. Suter, *Macromolecules* **1985**, *18*, 1467.
[24] G. J. Martyna, M. E. Tuckerman, D. J. Tobias, M. L. Klein, *Mol. Phys.* **1996**, *87*, 1117.
[25] S. Plimpton, *J. Comput. Phys.* **1995**, *117*, 1.
[26] P. A. Rodgers, *J. Appl. Polym. Sci.* **1993**, *48*, 1061.
[27] [27a] O. Olabisi, R. Simha, *Macromolecules* **1975**, *8*, 206; [27b] O. Olabisi, R. Simha, *Macromolecules* **1975**, *8*, 211.
[28] J. W. Barlow, *Polym. Eng. Sci.* **1978**, *18*, 238.
[29] S. Beret, J. M. Prausnitz, *Macromolecules* **1975**, *8*, 536.
[30] D. R. Paul, A. T. DiBennedetto, *J. Polym. Sci. C* **1965**, *10*, 17.
[31] A. T. DiBenedetto, *J. Polym. Sci. A1* **1963**, *3*, 459.
[32] G. D. Smith, O. Borodin, D. Bedrov, W. Paul, X. H. Qiu, M. D. Ediger, *Macromolecules* **2001**, *34*, 5192.
[33] R. H. Valentine, J. D. Ferry, T. Homma, J. Ninomiya, *J. Polym. Sci. A* **1968**, *2*, 479.
[34] J. E. Anderson, D. D. Davis, W. P. Slichter, *Macromolecules* **1969**, *2*, 166.
[35] S. J. Antoniadis, C. T. Samara, D. N. Theodorou, *Macromolecules* **1998**, *31*, 7944.
[36] V. G. Mavrantzas, T. D. Boone, E. Zervopoulou, D. N. Theodorou, *Macromolecules* **1999**, *32*, 5072.
[37] L. J. Fetters, D. J. Lohse, D. Richter, T. A. Witten, A. Zirkel, *Macromolecules* **1994**, *27*, 4639.
[38] D. Bedrov, G. D. Smith, W. Paul, *Phys. Rev. E* **2004**, *70*, 011804.
[39] B. Frick, D. Richter, C. L. Ritter, *Europhys. Lett.* **1989**, *9*, 557.
[40] D. Richter, B. Frick, B. Farago, *Phys. Rev. Lett.* **1988**, *61*, 2465.
[41] C. J. Pings, J. Wase, *J. Phys. Chem.* **1968**, *48*, 3016.
[42] D. W. Van Krevelen, "*Properties of Polymers: Their Estimation and Correlation with Chemical Structure*", Elsevier Science, Amsterdam 1990.
[43] A. Narros, A. Arbe, F. Alvarez, J. Colmenero, R. Zorn, W. Schweika, D. Richter, *Macromolecules* **2005**, *38*, 9847.
[44] [44a] M. L. Greenfield, D. N. Theodorou, *Macromolecules* **1993**, *26*, 5461; [44b] M. L. Greenfield, D. N. Theodorou, *Macromolecules* **1998**, *31*, 7068.
[45] V. A. Harmandaris, M. Doxastakis, V. G. Mavrantzas, D. N. Theodorou, *J. Chem. Phys.* **2002**, *116*, 436.
[46] N. C. Karayiannis, V. G. Mavrantzas, D. N. Theodorou, *Macromolecules* **2004**, *37*, 2978.

